References and Notes

1. N. W. Ashcroft, *Phys. World* **8**, 43 (July 1995).
2. E. Wigner and H. B. Huntington, *J. Chem. Phys.* **3**, 764 (1935); C. Friedli and N. W. Ashcroft, *Phys. Rev. B* **16**, 662 (1977); T. W. Barbee *et al.*, *Phys. Rev. Lett.* **62**, 1150 (1989); H. Chacham and S. G. Louie, *ibid.* **66**, 10963 (1991).
3. J. H. Eggert *et al.*, *Phys. Rev. Lett.* **66**, 671 (1991); C. Narayana, H. Luo, J. Orloff, A. L. Ruoff, *Nature* **393**, 46 (1998).
4. S. T. Weir, A. C. Mitchell, W. J. Nellis, *Phys. Rev. Lett.* **76**, 1860 (1996).
5. H. M. Van Horn, *Science* **252**, 384 (1991).
6. R. Smoluchowski, *Nature* **215**, 691 (1967); W. B. Hubbard, *Science* **214**, 145 (1981); G. Chabrier, D. Saumon, W. B. Hubbard, J. I. Lunine, *Astrophys. J.* **391**, 817 (1992); W. J. Nellis, M. Ross, N. C. Holmes, *Science* **269**, 1249 (1995).
7. D. Saumon *et al.*, *Astrophys. J.* **460**, 993 (1996).
8. D. Saumon, W. B. Hubbard, G. Chabrier, H. M. Van Horn, *ibid.* **391**, 827 (1992).
9. W. B. Hubbard *et al.*, *Phys. Plasmas* **4**, 2011 (1997).
10. G. Chabrier and I. Baraffe, *Astron. Astrophys.* **327**, 1039 (1997).
11. S. W. Haan *et al.*, *Phys. Plasmas* **2**, 2480 (1995); J. D. Lindl, *ibid.*, p. 3933; S. Nakai and H. Takabe, *Rep. Prog. Phys.* **59**, 1071 (1996).
12. The Hugoniot is the locus of density, pressure, and energy states in a material after passage of a single shock. It is a well-defined curve on the EOS surface. The compression (ratio of shocked to unshocked density) generally increases with pressure and approaches a value of 4 for an ideal gas in the high-pressure limit. The ratio can be greater than 4 when accounting for endothermic processes such as molecular excitations, dissociation, or ionization. At pressures above where these processes are complete, the compression must approach the ideal gas limit. EOSs for hydrogen isotopes are identical except for a scale factor in density.
13. G. I. Kerley, "A theoretical equation of state for deuterium" (Los Alamos Laboratory Rep. LA-4776, Los Alamos, NM, 1972); *J. Chem. Phys.* **73**, 460 (1980).
14. M. Ross, F. H. Ree, D. A. Young, *J. Chem. Phys.* **79**, 1487 (1983).
15. M Ross, *Phys. Rev. B* **58**, 669 (1998).
16. D. Saumon and G. Chabrier, *Phys. Rev A* **44**, 5122 (1991); **46**, 2084 (1992); *Phys. Rev. Lett.* **62**, 2397 (1989).
17. W. R. Magro, D. M. Ceperley, C. Pierleoni, B. Bernu, *Phys. Rev. Lett.* **76**, 1240 (1996); B. Militzer, W. Magro, D. Ceperley, in *Strongly Coupled Coulomb Systems*, G. J. Kalman, K. B. Blagoev, J. M. Rommel, Eds. (Plenum, New York, 1998).
18. H. Reinholz, R. Redmer, S. Nagel, *Phys. Rev. E* **52**, 5368 (1995).
19. W. J. Nellis *et al.*, *J. Chem. Phys.* **79**, 1480 (1983).
20. N. C. Holmes, M. Ross, W. J. Nellis, *Phys. Rev. B* **52**, 15835 (1995).
21. L. B. Da Silva *et al.*, *Phys. Rev. Lett.* **78**, 483 (1997).
22. E. M. Campbell, *Laser Part. Beams* **9**, 209 (1991).
23. Y. M. Gupta and S. M. Sharma, *Science* **277**, 909 (1997).
24. L. M. Barker and R. E. Hollenbach, *J. Appl. Phys.* **43**, 4669 (1972). VISAR, velocity interferometer system for any reflector, is a common term for this technique. These are the first VISAR measurements of shock velocity from a reflecting shock front in motion.
25. F. J. Rogers, *Astrophys. J.* **310**, 723 (1986); ———, F. J. Swenson, C. A. Iglesias, *ibid.* **456**, 902 (1996).
26. T. J. Lenosky, J. D. Kress, L. A. Collins, *Phys. Rev. B* **56**, 5164 (1997).
27. D. Saumon, G. Chabrier, H. M. Van Horn, *Astrophys. J. Suppl. Ser.* **99**, 713 (1995).

28. We thank N. W. Ashcroft, D. M. Ceperley, G. Chabrier, Y. M. Gupta, A. U. Hazi, N. C. Holmes, J. D. Johnson, G. I. Kerley, W. J. Nellis, M. Ross, F. J. Rogers, D. Saumon, T. Tajima, and D. A. Young for informative discussions and J. R. Asay, B. A. Hammel, J. D. Kilkenny, and L. G. Wiley for advice and support. This work was performed under the auspices of the U.S. Department of Energy by Lawrence Livermore National Laboratory under contract number W-7405-Eng-48.

22 April 1998; accepted 10 July 1998

Dimensionality-Driven Insulator-to-Metal Transition in the Bechgaard Salts

V. Vescoli, L. Degiorgi, W. Henderson, G. Grüner, K. P. Starkey, L. K. Montgomery

Optical experiments were conducted on a series of organic linear chain conductors with different values of the interchain single-electron transfer integral t_b, which quantifies the degree of anisotropy. Electron-electron interactions together with Umklapp scattering resulted in a correlation gap and an insulating state for small t_b. An insulator-to-metal transition was observed when t_b exceeded a critical value, on the order of the correlation gap E_{gap}. The absence of a plasma edge on the insulator side of the transition for polarization perpendicular to the chains suggests that the electrons are confined to the chains. The optical features of the metallic state, when contrasted with the magnetic properties, are suggestive of spin-charge separation.

Interacting electrons in reduced dimensions exhibit an enhanced tendency toward the formation of various broken symmetry ground states, whose properties have been explored by various techniques. The "normal" state, that is, the state at temperatures above the transition temperatures of the broken symmetry states, is of interest in part because a strictly one-dimensional (1D) interacting electron system cannot be described by Fermi liquid (FL) theory, the framework of which has been the cornerstone of the theory of interacting electrons in metals and semiconductors for the last half century. The theory is based on the recognition that when interactions can be treated as a perturbation, the low-lying excitations of an interacting electron gas are the same as those of the noninteracting case, only with the energy scales renormalized. FL theory has been thoroughly tested on a variety of materials and is usually valid in higher than one dimension; one well-known exception is the normal state of the two-dimensional (2D) copper oxide–based high-temperature superconductors. The 1D state predicted by the Tomonaga-Luttinger liquid (TLL) theory (*1*) is characterized by features such as spin-charge separation and the absence of a sharp edge in the distribution function at the Fermi wave vector $\mathbf{k}_F$. It has also been suggested (*2*) that for a small transfer integral between chains of interacting electrons, a new state of matter may emerge where the low-lying excitations are confined to the chains and single-electron interchain transfer is not possible but where tunneling of pairs may occur. An analogous scenario has been suggested to occur in high-temperature superconductors. Additional interesting effects arise when the lattice periodicity is involved (*3*, *4*). In this case, electron-electron interactions together with Umklapp scattering result in a correlation gap in the charge excitation spectrum for commensurate band filling (that is, for electron density per unit cell $n = p/q$ with p and q integers). The appearance of this gap also has a marked influence on the interchain electron transfer and on confinement.

The isostructural conductors, based on linear chains of the organic molecules tetramethyltetrathiafulvalene (TMTTF) and tetramethyltetraselenafulvalene (TMTSF), with different interchain counterions X (such as PF_6, ClO_4, and Br), have been the subject of intensive studies recently, to a large extent because of the novel concepts described above. Shortly after they were first synthesized by Bechgaard in 1979, they were found to undergo transitions to various broken symmetry ground states (such as antiferromagnetic, spin density wave, and superconducting states) at low temperatures, typically below 20 K (*4*). The states above the transition temperature, which we will refer to as T_{tr}, are unusual. For example, the resistivity ρ of the $(TMTTF)_2X$ salts has a minimum at a temperature T_ρ, which is in the range ~100 to 300 K. Below T_ρ, but above T_{tr}, ρ increases with decreasing T. In contrast, the

V. Vescoli and L. Degiorgi, Laboratorium für Festkörperphysik, Eidgenössische Technische Hochschule, CH-8093 Zürich, Switzerland. W. Henderson and G. Grüner, Department of Physics, University of California, Los Angeles, CA 90095–1547, USA. K. P. Starkey and L. K. Montgomery, Department of Chemistry, University of Indiana, Bloomington, IN 47405, USA.

$(TMTSF)_2X$ analogs display a metallic character (that is, a monotonic decrease of ρ with decreasing T) for $T > T_{tr}$. In both groups of salts, the magnetic susceptibility is weakly T-dependent for $T > T_{tr}$.

Because of a full charge transfer of one electron from the chains to each of the counterions, the band involving the chains is a quarter-filled hole band. A small amount of dimerization occurs along the chain direction (*4*), which splits the band into two bands, one empty and one half-filled. In the absence of electron-electron interactions, both a half- and a quarter-filled band result in a metallic state. However, in both cases, on-site and nearest neighbor Coulomb interactions result in a correlation gap (*5–7*), E_{gap}. Whether a half- or quarter-filled scenario is a more appropriate description for the Bechgaard salts is still being debated. However, this issue will not affect the forthcoming analysis or our conclusions, because in all cases E_{gap} refers to the minimum energy required to make a charge excitation in a system that would be gapless in the absence of correlation effects, and the concept can therefore be used in a general sense. Calculations and various experiments (*8–10*) have established the highly anisotropic band structure that is expected on the basis of structural characteristics. The transfer integrals in the b and c crystallographic directions (*11*), t_b and t_c, are different from each other, with t_b substantially greater than t_c. The small value of t_c suggests that at temperatures above about 10 K $\sim t_c/k_B$ (where k_B is the Boltzmann constant), which is the temperature range of interest in this report, the problem is essentially 2D, because thermal fluctuations destroy coherent transport that would result in weak three dimensionality at temperatures $T < t_c/k_B$.

The insulating state of the $(TMTTF)_2X$ salts has been interpreted in terms of a correlation gap, and the unusual properties of both the $(TMTTF)_2X$ and $(TMTSF)_2X$ salts were related to the TLL description before (*5*). The issue is, however, highly controversial; in fact, it has been argued (*12*) that the transport properties of the metallic state of the TMTSF analogs can be accounted for in terms of a weakly interacting FL. To address these issues, we conducted optical experiments over a wide spectral range on various examples of the Bechgaard salts. Our studies give clear evidence that (i) a crossover between insulating and conducting states occurs with increasing interchain charge transfer, and this transfer occurs when the unrenormalized transfer integral perpendicular to the chains is greater than E_{gap}, (ii) this crossover is accompanied by the appearance of a well-defined plasma frequency in the b' direction, which may be regarded as evidence of single-electron deconfinement, and (iii) the "metallic" state is highly unusual: Most of the spectral weight is associated with gapped charge excitations, and the frequency ω dependence of the conductivity (for $E_{gap} < \omega < 4t_a$) is consistent with the predictions of TLL theory. Furthermore, a comparison of the optical properties to the magnetic susceptibility suggests a metallic state with separation of the charge and spin excitations.

Crystals were grown by electrolytic methods, with currents adjusted so as to result in large single crystals (*13*). The optical reflectivity was measured in a broad frequency range for the electric field **E** polarized both along the a axis and along the b' axis (*11*). We have also evaluated the transport and dielectric properties at 100 GHz along the chains using a resonant technique (*14*).

The optical results presented here are in broad agreement with previous, less detailed studies (*15*, *16*), and they include frequencies below the conventional optical spectral range. Our results on the $(TMTSF)_2X$ salts were reported in recent works (*17*, *18*); here, we include data on $(TMTTF)_2X$ salts as well. The various experiments, when taken together, establish a gap for the charge excitations in the $(TMTTF)_2X$ salts and a gap feature together with a zero-frequency mode for the $(TMTSF)_2X$ salts.

The optical reflectivity measured in all salts for both polarizations is displayed in Fig. 1. In all cases, $T > T_{tr}$. We performed a standard Kramers-Kronig analysis to obtain the conductivity ($\sigma = \sigma_1 + i\sigma_2$) from the reflectivity. The real part of the conductivity σ_1 for the electric field polarized along the chains is shown in Fig. 2. The optical conductivity of the $(TMTTF)_2PF_6$ salt displays several transitions with large absorption features due to lattice vibra-

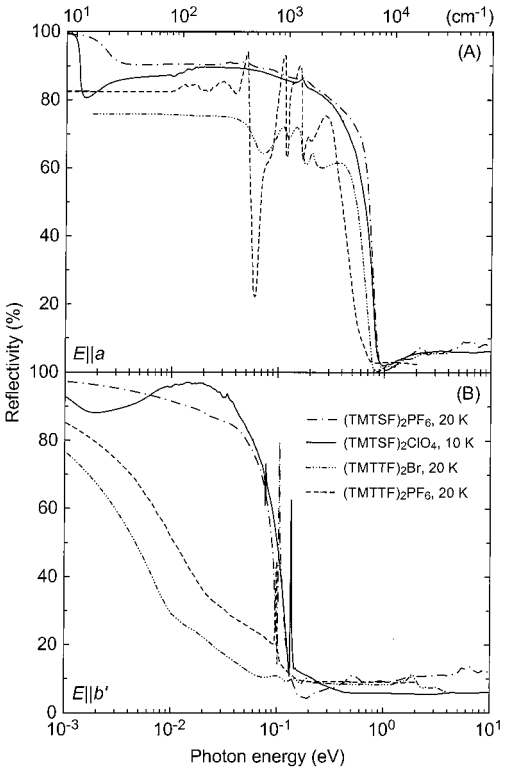

Fig. 1 (left). Optical reflectivity measured with the electric field polarized along **(A)** the a direction and **(B)** the b' direction, for temperatures above the phase transitions to the broken symmetry ground states in the $(TMTTF)_2X$ and $(TMTSF)_2X$ salts. The counterions are indicated in the figure. In the case of **E** polarized along the b' direction, no plasma edge is observed for the $(TMTTF)_2X$ salts, but it is present for the $(TMTSF)_2X$ salts. **Fig. 2 (right).** On-chain optical conductivity of **(A)** $(TMTTF)_2PF_6$, **(B)** $(TMTTF)_2Br$, and **(C)** $(TMTSF)_2X$ salts above the transitions to the broken symmetry states. The arrows indicate the gaps observed by dielectric response (E^{ε}_{gap}), dc resistivity (E^{dc}_{gap}), and photoemission (E^{ph}_{gap}).

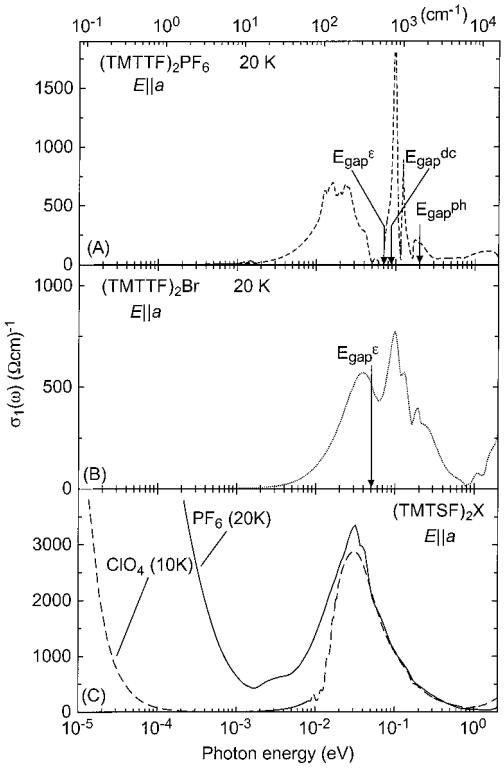

tions. Although it is clear that the optical properties are that of a semiconductor, with a gap for the charge excitations, evaluation of the magnitude of the gap, based on the optical spectra, is highly problematic. Thus, the results of other measurements were used to evaluate the correlation gap. The dc conductivity (*19*) can be well fitted to the expression $\sigma_{dc} = \sigma_0 \exp[-E_{gap}/(2k_BT)]$, resulting in a value of $E_{gap} = 700$ cm^{-1} (*20*). The low-temperature dielectric constant (ε) measured at 100 GHz is 100, and use of the equation $\varepsilon = 1 + (\omega_p/E_{gap})^2$ (where ω_p is the plasma frequency) resulted in a value of 600 cm^{-1} for the gap. Photoemission experiments (*21*) result in a gap of 1600 cm^{-1}. All of these values indicate that the features in the conductivity around 300 cm^{-1} are not due to excitations across the correlation gap but are due to phonons—the conclusion also reached by Pedron *et al.* (*16*) in their analysis of the room-temperature optical spectra. These results also suggest that the feature in $\sigma_1(\omega)$ near 800 cm^{-1} is associated with E_{gap}; this is supported by the fact that this feature has the correct spectral weight (*22*). The different gap values obtained for $(TMTTF)_2PF_6$ are displayed in Fig. 2A. For the $(TMTTF)_2Br$ salt, both the measured dielectric constant, $\varepsilon = 500$, and the low-lying optical feature give similar values for E_{gap}, where the maximum of the optical conductivity at 400 cm^{-1} was taken to be the value of E_{gap} (*23*). Because the band is partially filled, the charge gap in both of the $(TMTTF)_2X$ salts is interaction induced.

The optical properties of the $(TMTSF)_2X$ analogs, for which the dc conductivity gives evidence for metallic behavior down to low temperatures [to the transition to the spin density wave state at $T_{SDW} = 11.5$ and 6 K for the $(TMTSF)_2PF_6$ and $(TMTSF)_2ClO_4$ salts, respectively], are markedly different from those of a simple metal. A well-defined gap feature around 200 cm^{-1} and a zero-frequency mode (*17*, *18*) are observed. The combined spectral weight of the two modes is in full agreement with the known carrier concentration of $n = 1.4 \times 10^{21}$ cm^{-3} and a band mass that is very close to the electron mass. For both $(TMTSF)_2X$ salts, the zero-frequency mode has a small spectral weight on the order of 1% of the total. Nevertheless, this mode is responsible for the large metallic conductivity.

The reflectivity, measured with the electric field polarized in the b' direction, is displayed in Fig. 1B. In contrast to the sharp plasma edge observed in all of the salts with **E** parallel to the chains, we found a well-defined plasma edge only in the $(TMTSF)_2X$ salts (and only at low temperatures). No such feature appears in the $(TMTTF)_2X$ analogs.

Next we discuss these findings and relate them to the theoretical concepts advanced for weakly coupled chains. There is a well-established order for t_b among the four salts investigated. The $(TMTTF)_2X$ analogs are more anisotropic, and the transfer integrals are approximately given by $t_a:t_b:t_c = 250:10:1$ meV (*4*). For the $(TMTSF)_2X$ analogs, the transfer integrals are about 250:25:1 meV. The values for both groups of salts are in broad agreement with tight-binding model calculations (*24*). However, band structure calculations do not have sufficient precision to distinguish between the interchain transfer integrals within the $(TMTTF)_2X$ and $(TMTSF)_2X$ groups. Because t_b increases substantially with increasing pressure, pressure-dependence studies can be used to arrive at the relative values of t_b. For example, among the $(TMTTF)_2X$ salts, weaker interchain coupling for $(TMTTF)_2PF_6$ than for $(TMTTF)_2Br$ was established by showing that applying enough pressure to the PF_6 salt results in properties that are virtually identical to those of the Br salt. Similar studies show that the $(TMTSF)_2ClO_4$ salt has stronger interchain coupling than $(TMTSF)_2PF_6$. Sufficient pressure also causes the $(TMTTF)_2Br$ salt to behave like $(TMTSF)_2PF_6$. To arrive at a scale for t_b, we took the calculated values as averages for the $(TMTSF)_2X$ and $(TMTTF)_2X$ salts, respectively, and assumed that pressure changes t_b in a linear fashion. The positions of the various salts along the horizontal axis of Fig. 3 reflect this choice, with pressure values taken from the literature; such a scale has been widely used when discussing the broken symmetry ground states of these materials (*4*).

The solid line in Fig. 3 represents the overall behavior of the correlation gap. The decrease going from the $(TMTTF)_2X$ to the $(TMTSF)_2X$ analogs may represent various factors (*6*), such as the decreasing degree of dimerization and the slight increase in the bandwidth along the chain direction [as evidenced by the greater value of the plasma frequency measured along the chain direction in the $(TMTSF)_2X$ salts (*15*, *16*, *25*)]. The dashed line representing $2t_b$ (this is half the bandwidth in the tight-binding approximation) crosses the full line displaying the behavior of E_{gap} between the salts exhibiting insulating and metallic behavior, whereas the dash-dotted line representing t_b crosses the solid line between the two metallic salts. Therefore, our experiments strongly suggest that a crossover from a nonconducting to a conducting state occurs when the unrenormalized single-particle transfer integral between the chains exceeds the correlation gap by a factor, A, which is on the order of but somewhat greater than 1.

Additional evidence for a pronounced qualitative difference between states with $At_b < E_{gap}$ and $At_b > E_{gap}$ is given by plasma frequency studies along the b' direction. As is evident from Fig. 1B, there is no well-defined plasma frequency for the insulating state, and we regard this as evidence for the confinement (*26*) of electrons on individual chains. Conversely, the electrons become deconfined as soon as $At_b \sim E_{gap}$. This conclusion is not entirely unexpected: A simple argument (the same as one would advance for a band-crossing transition for an uncorrelated band semiconductor) would suggest that to create an electron hole pair with the electron and hole residing on neighboring chains, an energy comparable to the gap would be required. Several theories (*7*, *26*, *27*) suggest a strong renormalization of the relevant interchain transfer integral for coupled Luttinger liquids. These studies, however, do not take into account the periodicity of the underlying lattice and the resulting Umklapp scattering. Such scattering has a marked influ-

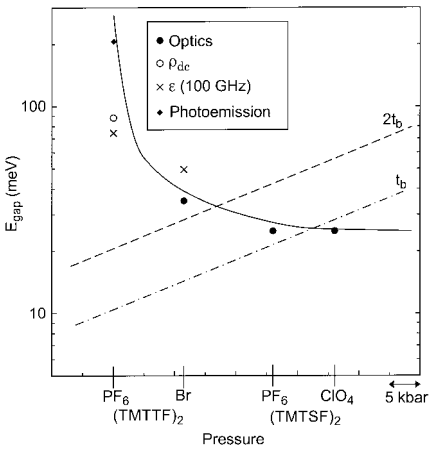

Fig. 3. The correlation gap as established by optics and other methods and the transfer integral, perpendicular to the chains, t_b for the $(TMTTF)_2X$ and $(TMTSF)_2X$ salts studied. The horizontal scale was derived with the results of pressure studies, as explained in the text. The dash-dotted (t_b) and dashed ($2t_b$) lines indicate the trend for the pressure dependence of the transfer integral.

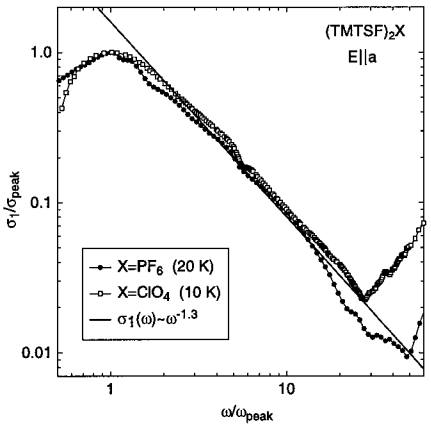

Fig. 4. The frequency dependence of the conductivity of the finite energy mode in the $(TMTSF)_2X$ salts. The solid line is Eq. 1 with the exponent $\gamma = 1.3$.

ence on the effect of interchain transfer. Renormalization group treatment (*28*) of two coupled Hubbard chains results in a crossover between confinement (that is, no interchain single-electron charge transfer) and deconfinement, at $At_b = E_{gap}$, with the value of A estimated to be between 1.8 and 2.3.

A transition or crossover from an insulator to a metal has also been conjectured by Bourbonnais (*29*), on the basis of studies of arrays of coupled chains. As the transition from confined (insulating) to deconfined (metallic) states (Fig. 3) occurs somewhere between $(TMTTF)_2Br$ (with $t_b \sim E_{gap}/2$) and $(TMTSF)_2PF_6$ (with $t_b \sim E_{gap}$), we regard the agreement between theory and experiment to be excellent. It has also been suggested (*18*, *30*), that a renormalized transfer integral t_b^{eff}, substantially smaller than t_b, is the relevant energy scale; our experiments show that this is not the case. We also note that, in the absence of pressure-dependent optical studies, it remains to be determined whether the onset of the transverse plasma edge, which we observe going from the $(TMTTF)_2X$ to $(TMTSF)_2X$ salts, coincides with the insulator-to-metal transition found in transport (*31*) and nuclear magnetic resonance (NMR) measurements (*32*). Although optical experiments under pressure are difficult to conduct, studies of the pressure dependence of the dielectric constant, combined with dc transport data, could clarify this issue.

The existence of a gap feature in the metallic state, containing nearly all of the spectral weight, is at first sight similar to what is expected for a band-crossing transition for simple semiconductors, which would result in a semimetallic state. However, the nearly temperature-independent magnetic susceptibility (*4*), which gives strong evidence for a gapless spin excitation spectrum (this has often been interpreted as a Pauli susceptibility or as the susceptibility due to a large exchange interaction), demonstrates that the state is not a simple semimetal. The existence of a gap, or pseudogap in the charge excitations with the absence of a gap for spin excitations, indicates charge-spin separation in the metallic state. This charge-spin separation is distinct from that of a 1D TLL, in which both excitations are gapless but have different velocities. Here, Umklapp scattering resulted in gapped charge excitations. The nature of the metallic state may be close to that of a doped 1D Mott-Hubbard semiconductor (*33*), where, in this case, the interchain transfer resulted in deviations from half- (or quarter-) filling on each chain and therefore had an effect similar to doping. Indeed, calculations (*30*, *34*) based on doped Hubbard chains resulted in a gap feature and a zero-frequency mode with a small spectral weight.

Additional evidence for an unusual metallic state comes from the frequency dependence of the finite energy mode. At frequencies greater than t_b, interchain electron transfer is irrelevant and calculations based on the 1D Hubbard model should be appropriate. Such calculations result in a frequency-dependent conductivity for frequencies greater than E_{gap} (*30*):

$$\sigma_1 \propto \omega^{-\gamma} \quad (1)$$

For a semiconductor without correlations, γ is equal to 3. Our results for frequencies greater than both t_b and E_{gap} but less than the on-chain bandwidth $4t_a$, which are shown in Fig. 4, can be described with Eq. 1 with an exponent $\gamma = 1.3$ for both $(TMTSF)_2X$ compounds. This suggests that, at finite energies, 1D correlations result in renormalization of the density of states. The exponent can in principle be used to obtain the Luttinger liquid parameter K_ρ, which controls the decay of all correlation functions (*18*, *30*, *35*). From our value for γ and the assumption that quarter-filled band Umklapp scattering is dominant, we obtained $K_\rho \sim 0.23$ (*18*), which is in reasonable agreement with photoemission (*21*, *35*) and transport data (*31*).

Our experiments raise several important yet unresolved issues. The first is related to the relevance of calculations based on the doped 1D Hubbard model. In the calculations, the zero-energy mode is associated with doping-induced soliton excitations. Although interchain single-electron transfer between chains may also result in "self-doping" of individual chains, the nature of the low-lying excitations of coupled chains is not yet resolved. Second, although our experiments suggest an unusual frequency-dependent conductivity in the high-frequency 1D regime, whether the value of γ we obtain is in agreement with the parameter range given by the theoretical models remains to be seen. The third is related to concept of deconfinement. Although our experiments result in good overall agreement with calculations based on two coupled chains (*28*), it is unclear whether a theory involving an infinite network of chains results in the same condition for deconfinement (*29*). Moreover, we have not discussed temperature-dependent effects and the possibility of a crossover with increasing temperature to Luttinger liquid behavior at low frequency. The absence of a well-defined plasma frequency at room temperature may be related to such a crossover, which was inferred from NMR (*32*) and transport (*31*) studies.

References and Notes

1. J. Luttinger, *J. Math. Phys.* **4**, 1154 (1963); S. Tomonaga, *Prog. Theor. Phys.* **5**, 554 (1950); for a review, see H. J. Schulz, *Int. J. Mod. Phys. B* **5**, 57 (1991).
2. S. P. Strong, D. G. Clark, P. W. Anderson, *Phys. Rev. Lett.* **73**, 1007 (1994).
3. D. Jérome and L. G. Caron, Eds., *Proceedings of the NATO Study Institute on Low Dimensional Conductors and Superconductors*, vol. 155 (Plenum, New York, 1987).
4. D. Jérome and H. J. Schulz, *Adv. Phys.* **31**, 229 (1982); D. Jérome, in *Physics and Chemistry of Low Dimensional Inorganic Conductors*, *NATO ASI Series B*, C. Schlenker, J. Dumas, M. Greenblatt, S. Van Smaalen, Eds. (Plenum, New York, 1996), vol. 354, pp. 141–167.
5. For a review, see C. Bourbonnais, *Synth. Metals* **84**, 19 (1997).
6. K. Penc and F. Mila, *Phys. Rev. B* **50**, 11429 (1996).
7. F. Mila and D. Poilblanc, *Phys. Rev. Lett.* **76**, 287 (1996), and references therein.
8. P. M. Grant, *J. Phys.* **44**, C3 (1983).
9. L. Balicas *et al.*, *J. Phys. I* **4**, 1539 (1994).
10. B. J. Klemme *et al.*, *Phys. Rev. Lett.* **75**, 2408 (1995).
11. The b' and c' directions are perpendicular to the chain direction a. These directions also define the faces of the samples on which the optical experiments were conducted and are slightly different from the b and c directions of the unit cell because of the triclinic crystal structure. This small difference does not influence the arguments advanced in this work.
12. L. P. Gor'kov, *J. Phys. I* **6**, 1697 (1996); L. P. Gor'kov and M. Mochena, in preparation.
13. L. K. Montgomery, in *Organic Conductors: Fundamentals and Applications*, *Applied Physics Series*, J. P. Farges, Ed. (Dekker, New York, 1994), pp. 138–140.
14. S. Donovan, O. Klein, M. Dressel, K. Holczer, G. Grüner, *Int. J. Infrared Millimeter Waves* **14**, 2359 (1993).
15. C. S. Jacobsen, D. B. Tanner, K. Bechgaard, *Phys. Rev. Lett.* **46**, 1142 (1981); *Solid State Commun.* **38**, 423 (1981); *Phys. Rev. B* **28**, 7019 (1983).
16. D. Pedron, R. Bozio, M. Meneghetti, C. Pecile, *Phys. Rev. B* **49**, 10893 (1994).
17. M. Dressel, A. Schwartz, G. Grüner, L. Degiorgi, *Phys. Rev. Lett.* **77**, 398 (1996), and references therein.
18. A. Schwartz *et al.*, *Phys. Rev. B* **58**, 1261 (1998).
19. S. E. Brown, personal communication; M. Dressel, personal communication.
20. Throughout this work, we express both energy and frequency in units of inverse wavelength. 1 cm^{-1} is equivalent to 30 GHz or 0.125 meV.
21. F. Zwick *et al.*, *Phys. Rev. Lett.* **79**, 3982 (1997).
22. The spectral weight of the feature at 800 cm^{-1} is consistent with the observed plasma frequency of 6000 cm^{-1}, with the use of the relation $\int_0^\infty \sigma_1(\omega) d\omega = \omega_p^2/8$.
23. For a 1D semiconductor, the optical conductivity displays a maximum, which may be somewhat broadened by various effects, at the gap, justifying the assignment of the gap to the frequency at which the maximum in $\sigma_1(\omega)$ occurs.
24. L. Ducasse *et al.*, *J. Phys. C* **19**, 3805 (1986).
25. V. Vescoli *et al.*, in preparation.
26. P. W. Anderson, *Proc. Natl. Acad. Sci. U.S.A.* **92**, 6668 (1995).
27. C. Bourbonnais and L. G. Caron, *Int. J. Mod. Phys. B* **5**, 1033 (1991).
28. Y. Suzumura, M. Tsuchiizu, G. Grüner, *Phys. Rev. B* **57**, R15040 (1998).
29. C. Bourbonnais, in *Strongly Interacting Fermions and High T_c Superconductivity*, B. Doucot and J. Zinn-Justin, Eds. (Elsevier, Amsterdam, 1995), pp. 307–367.
30. T. Giamarchi, *Physica B Phys. Condensed Matter* **230–232**, 975 (1997), and references therein.
31. J. Moser *et al.*, *Eur. Phys. J. B* **1**, 39 (1998).
32. P. Wzietek *et al.*, *J. Phys. I* **3**, 171 (1993).
33. H. Mori, H. Fukuyama, I. Imada, *J. Phys. Soc. Jpn.* **63**, 1693 (1994).
34. N. Bulut, D. J. Scalapino, S. R. White, *Phys. Rev. Lett.* **72**, 705 (1994).
35. B. Dardel *et al.*, *Europhys. Lett.* **24**, 687 (1993).

36. We gratefully acknowledge useful discussions with S. Chakravarty, H. Fukuyama, T. Giamarchi, L. Gor'kov, D. Jérome, S. Kivelson, F. Mila, and Y. Suzumura. Research at Eidgenössische Technische Hochschule was supported by the Swiss National Foundation for Scientific Research. Research at University of California, Los Angeles, was supported by NSF grant DMR-9503009. Research at Indiana University was sponsored by NSF grant DMR-9414268.

20 April 1998; accepted 30 June 1998